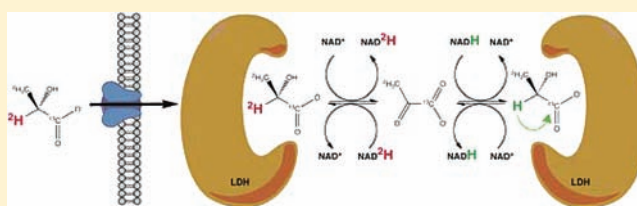


# Probing Lactate Dehydrogenase Activity in Tumors by Measuring Hydrogen/Deuterium Exchange in Hyperpolarized L-[1-<sup>13</sup>C,U-<sup>2</sup>H]Lactate

Brett W. C. Kennedy, Mikko I. Kettunen, De-En Hu, and Kevin M. Brindle\*

Department of Biochemistry, University of Cambridge, Tennis Court Road, Cambridge CB2 1GA, United Kingdom, and Cancer Research UK Cambridge Research Institute (CRI), Li Ka Shing Centre, Robinson Way, Cambridge, CB2 0RE, United Kingdom

**ABSTRACT:** <sup>13</sup>C magnetic resonance spectroscopy and spectroscopic imaging measurements of hyperpolarized <sup>13</sup>C label exchange between exogenously administered [1-<sup>13</sup>C]-pyruvate and endogenous lactate, catalyzed by lactate dehydrogenase (LDH), has proved to be a powerful approach for probing tissue metabolism in vivo. This experiment has clinical potential, particularly in oncology, where it could be used to assess tumor grade and response to treatment. A limitation of the method is that pyruvate must be administered in vivo at supra-physiological concentrations. This problem can be avoided by using hyperpolarized [1-<sup>13</sup>C]lactate, which can be used at physiological concentrations. However, sensitivity is limited in this case by the relatively small pyruvate pool size, which would result in only low levels of labeled pyruvate being observed even if there was complete label equilibration between the lactate and pyruvate pools. We demonstrate here a more sensitive method in which a doubly labeled lactate species can be used to measure LDH-catalyzed exchange in vivo. In this experiment exchange of the C2 deuterium label between injected hyperpolarized L-[1-<sup>13</sup>C,U-<sup>2</sup>H]lactate and endogenous unlabeled lactate is observed indirectly by monitoring phase modulation of the spin-coupled hyperpolarized <sup>13</sup>C signal in a heteronuclear <sup>1</sup>H/<sup>13</sup>C spin-echo experiment.



## INTRODUCTION

Dynamic nuclear polarization (DNP) of <sup>13</sup>C-labeled cell substrates, which enhances their sensitivity to detection in vivo by over 10,000-fold, has shown considerable promise for metabolic imaging in vivo, particularly in the field of cancer.<sup>1,2</sup> The most widely used substrate to date has been hyperpolarized [1-<sup>13</sup>C]pyruvate, which has been used for early noninvasive detection of tumor response to drug treatment<sup>3,4</sup> and assessment of tumor grade.<sup>5</sup> Intravenous injection of hyperpolarized [1-<sup>13</sup>C]pyruvate results in exchange of the hyperpolarized <sup>13</sup>C label with endogenous lactate in the reaction catalyzed by lactate dehydrogenase (E.C. 1.1.1.27) (LDH). Although there will be some net conversion of the injected pyruvate into lactate, the equilibrium constant for the reaction is such that chemical near-equilibrium is achieved with only a small net conversion of pyruvate into lactate (see Supporting Information in ref 3), which is then followed by exchange of the hyperpolarized <sup>13</sup>C label between the steady-state near-equilibrium pyruvate and lactate pools. The evidence that this is an exchange reaction, which is discussed in ref 2 is summarized in the following. LDH has long been known to catalyze a reaction that is near-to-equilibrium in the cell.<sup>6</sup> Addition of exogenous lactate has been shown to increase the isotope exchange velocity between pyruvate and lactate, increasing the detectable <sup>13</sup>C label in the lactate pool.<sup>3</sup> This is incompatible with net flux, where addition of lactate would result in product inhibition and a decrease in the rate of lactate labeling, but is consistent with isotope exchange, where the

resulting increase in the near-equilibrium NADH concentration stimulates the exchange velocity of the enzyme.<sup>7</sup> The exchange has been demonstrated directly in tumor cell suspensions by using [3-<sup>13</sup>C]pyruvate and unlabeled lactate and detecting the presence of the <sup>13</sup>C label in the methyl group via splitting of the methyl proton resonance due to <sup>13</sup>C-<sup>1</sup>H spin-spin coupling. The total pyruvate pool size remained relatively constant, while there was a decrease in the concentration of the <sup>13</sup>C-labeled species and an increase in the <sup>12</sup>C-labeled species. There were nearly reciprocal changes in the concentrations of the <sup>12</sup>C- and <sup>13</sup>C-labeled lactate species (see Supporting Information in 3). Exchange has also been demonstrated in vivo using magnetization transfer experiments in tumors displaying signals from hyperpolarized [1-<sup>13</sup>C]pyruvate and lactate following injection of a tumor-bearing animal with hyperpolarized [1-<sup>13</sup>C]pyruvate. Inversion of the lactate signal resulted in an increased rate of decay of the pyruvate resonance, demonstrating flux of hyperpolarized <sup>13</sup>C label from lactate into the pyruvate pool.<sup>8</sup> Recognizing that this is an exchange reaction explains observations made in vivo with hyperpolarized [1-<sup>13</sup>C]pyruvate. Thus, tumors show relatively high levels of lactate labeling since they tend to have large endogenous lactate pools, which provides a large pool for the label to exchange into and also increases the rate of the LDH-catalyzed reaction by increasing the NADH concentration.<sup>7</sup> Tumors also express high levels of

Received: January 9, 2012

Published: February 9, 2012

LDH-A, whose expression can be further increased by tumor hypoxia.<sup>9</sup> These correlations with LDH-A activity and lactate pool size can explain why lactate labeling is correlated with tumor grade.<sup>5</sup> Decreases in LDH activity and lactate and NAD(H) concentrations post-therapy also explain why measurements of the kinetics of lactate labeling following injection of hyperpolarized  $[1-^{13}\text{C}]$ pyruvate can be used to assess early treatment response in tumors.<sup>3,4,7</sup>

A potential limitation of the hyperpolarized  $[1-^{13}\text{C}]$ pyruvate experiment is that pyruvate is injected at supra-physiological concentrations. In preclinical studies pyruvate has been injected at a whole blood concentration of  $\sim 8$  mM,<sup>3</sup> assuming a mouse blood volume of 95 mL/kg,<sup>10</sup> whereas the physiological plasma pyruvate concentration is  $\sim 0.2$  mM.<sup>11</sup> In the first clinical trial of hyperpolarized  $[1-^{13}\text{C}]$ pyruvate, where the aim was to use it to detect treatment response in prostate cancer, pyruvate has been injected at 0.43 mL/kg of a 250 mM solution (ClinicalTrials.gov Identifier: NCT01229618), which equates to a whole blood concentration of  $\sim 1.5$  mM, assuming a blood volume of 70 mL/kg,<sup>12</sup> whereas the concentration of pyruvate in whole human blood from fasted individuals has been measured at  $0.061 \pm 0.024$  mM.<sup>13</sup> Although there has been no evidence of toxicity at these pyruvate concentrations, which is probably because the pyruvate clears quickly from the circulation, it would nevertheless be desirable to administer the labeled substrate at concentrations that are within the physiological range. Lactate is present in mouse plasma at  $\sim 4$  mM<sup>11</sup> and in human blood at  $0.92 \pm 0.26$  mM, although this can rise to much higher levels following exercise (1–5 mM);<sup>14</sup> therefore, monitoring lactate–pyruvate exchange using hyperpolarized  $[1-^{13}\text{C}]$ lactate should be a desirable option. The sensitivity of this experiment is limited, however, by the relatively small size of the pyruvate pool.<sup>15</sup> Thus, even if the exchange were very fast and there were complete label equilibration between the lactate and pyruvate pools within the lifetime of the hyperpolarized signal, the amount of detectable signal would be limited by the size of the pyruvate pool. Our solution to this problem is to use a doubly labeled lactate molecule,  $[1-^{13}\text{C},\text{U}-^2\text{H}]$ lactate, in which the LDH-catalyzed exchange of the deuterium label at the C2 position with endogenous unlabeled lactate (Figure 1) is monitored through phase

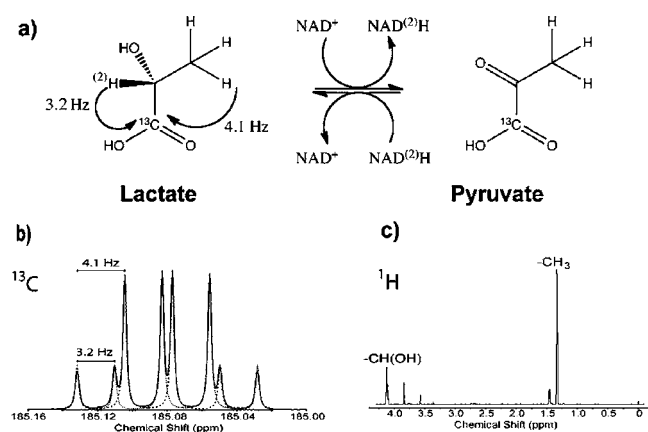


**Figure 1.** Oxidation of lactate and reduction of pyruvate in the reaction catalyzed by lactate dehydrogenase. The hydrogen that is exchanged for deuterium in lactate ( $^2\text{H}$ ) and the coupling constants for spin–spin coupling between the methylene and methyl protons and the  $^{13}\text{C}$  at the C1 position of lactate are indicated. The bottom row shows  $^{13}\text{C}$  and  $^1\text{H}$  spectra of  $L-[1-^{13}\text{C}]$ lactate.

modulation of the spin-coupled hyperpolarized  $^{13}\text{C}$  resonance in a heteronuclear  $^{13}\text{C}/^1\text{H}$  spin–echo experiment (Figure 2). Initially, exchange of deuterium will be between the two labeled lactate species,<sup>16</sup> although in the longer term the deuterium will exchange with solvent water.<sup>17</sup>

## METHODS

### Synthesis of $L-[1-^{13}\text{C}_1,2-^1\text{H}_3,3-^2\text{H}_3]$ , and $L-[1-^{13}\text{C}_1,\text{U}-^2\text{H}]$ Lactate.

The deuterated lactate species were prepared as described previously for  $L-[2-^1\text{H}_3,3-^2\text{H}_3]$  and  $L-[U-^2\text{H}]$ lactate.<sup>17,18</sup> Briefly, 1 g sodium  $L-[1-^{13}\text{C}_1]$ lactate (CIL, Massachusetts, USA or Sigma Aldrich, Gillingham, UK) as a 20% w/v solution in water was lyophilized and reconstituted in 85 mL  $\text{D}_2\text{O}$  containing 0.1 M sodium phosphate buffer ( $\text{pH}^* = 6.0$ ), 3 mM DTT, 0.5 mM disodium EDTA and 1.5 mM  $\text{NAD}^+$  (lithium salt), lactate dehydrogenase (1 kU, rabbit muscle, Sigma Aldrich, Gillingham, UK) and lipoamide dehydrogenase (75 U, pig heart, Calzyme, San Luis Obispo, CA, USA). The mixture was incubated at  $37^\circ\text{C}$  in the dark for 2 weeks, by which time  $>97\%$  of the C2 protons had exchanged for deuterons (by comparison of the  $^{13}\text{C}$  and  $^1\text{H}$  NMR integrals in fully relaxed spectra). The mixture was heated to  $100^\circ\text{C}$  for 10 min and the precipitated protein removed by filtration through a  $0.22\ \mu\text{m}$  pore size membrane. To the filtrate, 0.15 g (1.7 mmol)  $[1-^{13}\text{C}]$ pyruvic acid (CIL, Massachusetts, USA) was added with enough disodium phosphate to increase the phosphate concentration to 200 mM. The  $\text{pH}^*$  was raised to 7.7 with 9% w/v LiOD in  $\text{D}_2\text{O}$ ; 600 mg (0.9 mmol)  $\text{NAD}^+$  (lithium salt) and 1 kU of lactate dehydrogenase and glutamate–pyruvate transaminase (Roche, Burgess Hill, UK) were added. The mixture was incubated at  $37^\circ\text{C}$  in the dark for 2 weeks, after which time  $>96\%$  of the C3 protons had exchanged for deuterons. For the preparation of  $L-[1-^{13}\text{C}_1,3-^2\text{H}_3]$ lactate, sodium  $L-[1-^{13}\text{C}_1]$ lactate was incubated in this latter mixture.

The zinc salt of lactate was obtained by acidification of the solution with 32% HCl, followed by neutralization with basic zinc carbonate. The resulting zinc lactate was purified by recrystallization from water/ethanol. The sodium salt was prepared using an ion-exchange resin (Dowex 50Wx8,  $\text{Na}^+$  form) and then lyophilized. The lactate concentration was determined by enzymatic assay<sup>19</sup> and by  $^1\text{H}$  and  $^{13}\text{C}$  NMR spectroscopy. The lactate purity was  $\geq 90\%$ , and the yield was 73% for perdeuterated lactate and 75% for the  $[1-^{13}\text{C}_1,3-^2\text{H}_3]$ lactate.

**NMR Spectroscopy in Vitro.** Experiments were performed at 9.4 T using a vertical bore magnet (Oxford Instruments) interfaced to Varian  $^1\text{H}/^{13}\text{C}$  Inova console (Palo Alto) and a 10 mm  $^{13}\text{C}/^1\text{H}$  probe. A  $^{13}\text{C}/^1\text{H}$  heteronuclear spin–echo experiment was used with a 4 ms adiabatic  $^{13}\text{C}$  BIR4  $180^\circ$  refocusing pulse<sup>20</sup> followed immediately by a 10 ms hyperbolic secant ( $R = 10$ )  $^1\text{H}$  inversion pulse with the power adjusted either to zero or optimized to provide adiabatic inversion (Figure 2). The excitation profile of the  $^1\text{H}$  pulse was centered at 4.11 ppm, in order to selectively invert the C2 resonance without disturbing the C3 resonance at 1.33 ppm. The experiment was also performed with the  $^1\text{H}$  excitation profile centered at 1.33 ppm. A series of spectra, with echo times varying between 50 and 600 ms, were acquired into 2048 complex points with an 8 kHz spectral width and a repetition time of 180 s. The  $^{13}\text{C}$   $T_1$ 's and  $T_2$ 's were measured at thermal equilibrium using inversion recovery and Carr–Purcell–Meiboom–Gill pulse sequences respectively.

**Hyperpolarization of  $L-[1-^{13}\text{C}_1]$ ,  $L-[1-^{13}\text{C}_1,2-^1\text{H}_3,3-^2\text{H}_3]$ , and  $L-[1-^{13}\text{C}_1,\text{U}-^2\text{H}]$ Lactate and  $[1-^{13}\text{C}]$ Pyruvate.** To aqueous solutions of  $L-[1-^{13}\text{C}_1]$ ,  $[1-^{13}\text{C}_1,2-^1\text{H}_3,3-^2\text{H}_3]$ , or  $[1-^{13}\text{C}_1,\text{U}-^2\text{H}]$ sodium lactate ( $\sim 50\%$  w/v) were added trityl radical (OX063; GE Healthcare, Amersham, UK) and gadolinium chelate (Dotarem; Guerbet, Roissy, France) to final concentrations of 15 mM and 1.2 mM, respectively. DMSO, to a final concentration of 30% w/v, was present in order to ensure glass formation in the solid state.  $[1-^{13}\text{C}]$ Pyruvic acid samples (44 mg) contained 15 mM trityl radical and 1.4 mM of a gadolinium chelate (Dotarem). Samples were hyperpolarized as described previously.<sup>3</sup> Briefly, the sample was frozen rapidly under liquid helium at 3.35 T in an alpha-prototype hyperpolarizer (GE Healthcare Plc, Amersham, UK) at a pressure of  $\sim 1$  mbar ( $\sim 1.2$  K). Polarization was transferred to the  $^{13}\text{C}$  nuclei with irradiation at 93.965 GHz (100 mW)

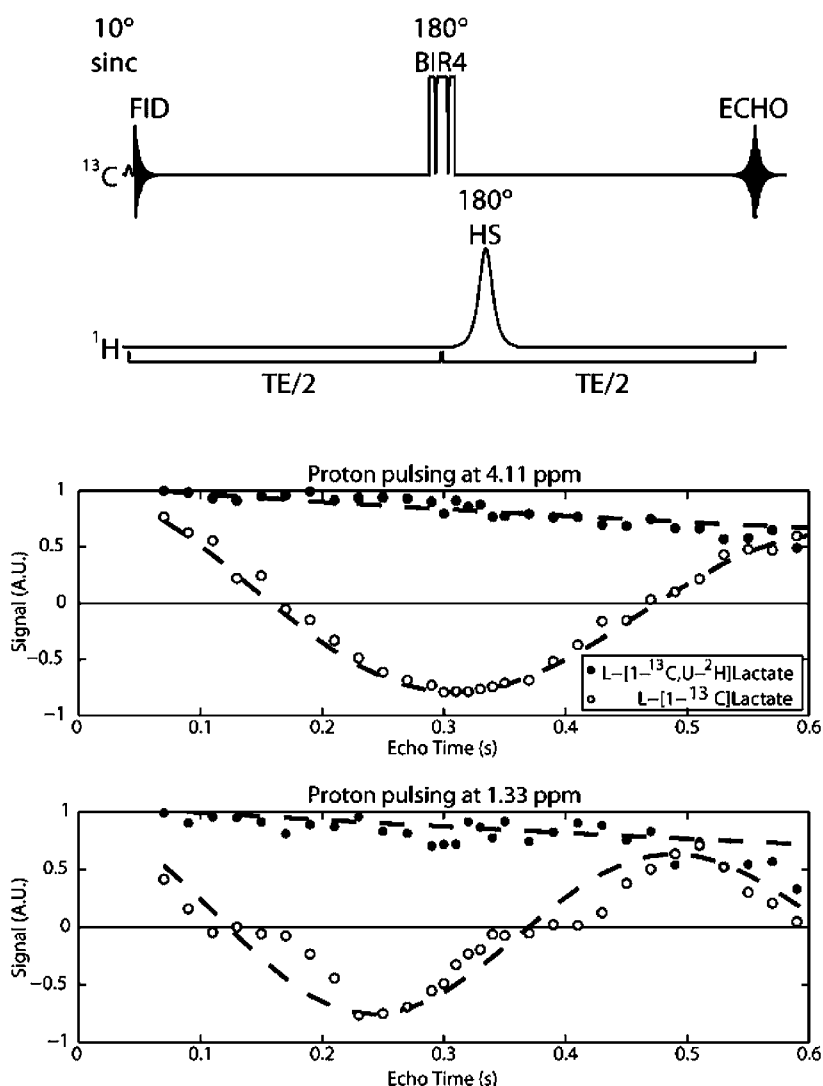


**Figure 2.**  $^{13}\text{C}/^1\text{H}$  Heteronuclear spin–echo experiment with  $L$ - $[1-^{13}\text{C}]$ lactate and  $L$ - $[1-^{13}\text{C},\text{U}-^2\text{H}]$ lactate at thermal equilibrium. Signal intensity is plotted versus echo time (TE). Frequency-selective  $180^\circ$   $^1\text{H}$  pulses were applied at 4.11 ppm and at 1.33 ppm.

over 90 min for lactate and 45 min for pyruvate. For both substrates the levels of polarization were typically greater than 20%. Lactate samples were dissolved in 4 mL PBS at  $180^\circ\text{C}$  and 10 bar to give a concentration of 60 mM and pyruvate samples were dissolved in 6 mL of HEPES buffer (40 mM HEPES, 94 mM NaOH, 30 mM NaCl and 100 mg/L EDTA) at  $180^\circ\text{C}$  and 10 bar to give a concentration of 75 mM. The samples were cooled before 0.2 mL was injected within 10 s either into a 10 mm NMR tube or into a C57BL/6 mouse via a tail-vein catheter.

**Tumor Experiments.** Female C57BL/6 mice ( $n = 4, 6$ –8 weeks of age; Charles River Ltd., Margate, UK) were injected subcutaneously in the lower flank with  $5 \times 10^6$  EL-4 cells (EL-4 is a murine lymphoma cell line). At this location there was no detectable respiratory motion in MR images. MRS was performed when the tumors had grown to a size of  $\sim 2\text{ cm}^3$  (which was reached typically at 10 days following implantation).<sup>3</sup> One of the animals was treated with an intraperitoneal injection of 67 mg etoposide (PCH Pharmachemie BV) per kg body weight 24 h after the first MRS experiment, and the MRS measurement was repeated 24 h after treatment. For MRS experiments, animals were anesthetized with intraperitoneal injections of Hypnorm (VetaPharma, Leeds, UK)/Hypnovel (Roche, Welwyn Garden City, UK)/dextrose–saline (4%:0.18%) in a 5:4:31 ratio (10 mL/kg body weight), and a catheter was inserted into the tail vein for injection of hyperpolarized lactate or pyruvate. The body temperature of the

animals was maintained by blowing warm air through the magnet bore. All experiments were conducted in compliance with a project license and personal licenses issued under the Animals (Scientific Procedures) Act of 1986 and were designed with reference to the United Kingdom Co-ordinating Committee on Cancer Research guidelines for the welfare of animals in experimental neoplasia. The work was approved by a local ethical review committee.

**MR Spectroscopy in Vivo.** Experiments were performed using a 9.4 T vertical bore magnet (Oxford Instruments) interfaced to a Varian  $^{\text{Unity}}$ Inova console (Palo Alto). A  $^{13}\text{C}$ -surface coil (diameter 24 mm) was placed directly over the tumor, and the animal holder was then placed inside a  $^1\text{H}$  volume coil (Millipede, Varian Inc., length 6 cm, diameter 4 cm). Transverse  $^1\text{H}$  scout images were acquired using a gradient-echo pulse sequence ( $30^\circ$  pulse; repetition time (TR), 300 ms; echo time (TE), 2.2 ms; field-of-view (FOV)  $35\text{ mm} \times 35\text{ mm}$  in a data matrix of  $256 \times 256$  with two averages per increment; slice thickness 2 mm and 21 transverse slices).  $^{13}\text{C}$  Data collection was started 8 s after the beginning of a 200  $\mu\text{L}$  i.v. injection of either 60 mM hyperpolarized  $[1-^{13}\text{C},\text{U}-^2\text{H}]$ lactate or  $[1-^{13}\text{C}]$ lactate or 75 mM hyperpolarized  $[1-^{13}\text{C}]$ pyruvate and was continued for 75 s. Spectra were acquired, in the case of pyruvate, using a nominal flip angle of  $10^\circ$  at intervals of 1 s and in the case of lactate using a heteronuclear  $^{13}\text{C}/^1\text{H}$  spin–echo experiment which consisted of pairs of spin–echo spectra, echo time 310 ms, collected with and without an

$^1\text{H}$  inversion pulse ( $H_+/H_-$ ) with a 500 ms delay between the low flip angle pulse of each member of the pair and a 5.5 s delay between the pairs. The spin-echo pulse sequence consisted of a nonselective  $^{13}\text{C}$  excitation pulse, with a  $10^\circ$  nominal flip angle, a 4 ms adiabatic  $^{13}\text{C}$  BIR4  $180^\circ$  refocusing pulse,<sup>20</sup> followed immediately by a 10 ms hyperbolic secant ( $R = 10$ )  $^1\text{H}$  inversion pulse centered at 4.11 ppm with the power adjusted either to 0 ( $H_-$ ) or optimized to provide adiabatic inversion ( $H_+$ ) (Figure 2). The phase of the excitation pulse was changed by  $180^\circ$  for the second member of each echo pair to account for inversion of the remaining longitudinal magnetization following the previous  $^{13}\text{C}$  refocusing pulse. Crusher gradients (5 G/cm, 2.5 ms) were placed around the refocusing pulses to destroy unwanted coherences. Data were acquired from the spin-echoes (spectral width 8000 Hz, 512 complex points centered on the echo maximum) and also from the free-induction decay (FID) obtained 1 ms after the excitation pulse (acquisition time 1 ms, spectral width 8000 Hz, 512 complex points) to assess the loss of longitudinal magnetization within the echo pair. The order of the proton pulses within the echo pairs ( $H_+/H_-$  or  $H_-/H_+$ ) was also changed in some experiments. At the end of the isotope exchange measurements, at  $\sim 80$  s after lactate injection, apparent  $T_2$  relaxation times were measured using a multiecho sequence, with an echo-spacing of 14 ms. Only even echoes were used for  $T_2$  analysis. In a separate group of animals, apparent  $R_1$  relaxation rates were measured using a pulse-acquire sequence with a  $10^\circ$  nominal flip angle,  $^{13}\text{C}$  pulse, and 10 s repetition time (acquisition time 1 ms, spectral width 8000 Hz, 768 complex points).

**Kinetic Analysis.** Lactate peak integrals were calculated from phase- and baseline-corrected spectra. The intensities of the deuterated ( $S_{\text{DL}}$ ) and protonated ( $S_{\text{HL}}$ ) lactate signals were calculated from the spin-echo signal intensities within each pair of echoes as:

$$S_{\text{DL}} = \frac{S_{\text{H-}} + S_{\text{H+}}}{2} \quad (1)$$

$$S_{\text{HL}} = \frac{S_{\text{H-}} - S_{\text{H+}}}{2} \quad (2)$$

where  $S_{\text{H-}}$  and  $S_{\text{H+}}$  are echo intensities measured in the absence and presence of the  $^1\text{H}$  pulses, respectively. These equations were modified to account for the effect of imperfect inversion of the  $^1\text{H}$ -coupled  $^{13}\text{C}$  resonance following application of a  $180^\circ$   $^1\text{H}$  pulse:

$$S_{\text{DL}} = \frac{FS_{\text{H-}} + S_{\text{H+}}}{1 + F} \quad (3)$$

$$S_{\text{HL}} = \frac{S_{\text{H-}} - S_{\text{H+}}}{1 + F} \quad (4)$$

where  $F$  is the fraction of inversion, with 1.0 being complete inversion. In experiments with C2-protonated lactate ( $L-[1-^{13}\text{C}]$ lactate) the value of  $F$  was determined to be 0.88.

The data were fitted initially to a simple two-site exchange model<sup>3</sup> to obtain the rate constants describing label flux from C2-deuterated to C2-protonated lactate ( $k_{\text{DH}}$ ) and from C2-protonated to C2-deuterated lactate ( $k_{\text{HD}}$ ) and the longitudinal relaxation rates for the deuterated ( $\rho_{\text{D}}$ ) and protonated lactate ( $\rho_{\text{H}}$ ) species. The relaxation rates were assumed to be identical for both species (see Table 2).

$$\begin{bmatrix} S_{\text{DL}} \\ S_{\text{HL}} \end{bmatrix}_t = e^{\left( \begin{bmatrix} -(k_{\text{DH}} + \rho_{\text{D}}) & k_{\text{HD}} \\ k_{\text{DH}} & -(k_{\text{HD}} + \rho_{\text{H}}) \end{bmatrix} t \right)} \begin{bmatrix} S_{\text{DL}} \\ S_{\text{HL}} \end{bmatrix}_0 \quad (5)$$

The apparent  $R_1$  relaxation rates were also calculated, using eq 6, from pulse-acquire data (see above) and from the FID obtained immediately following the excitation pulse in the spin-echo experiments.

$$S_t = S_0 e^{(-\rho t)} \quad (6)$$

Both the echo and FID intensities were corrected for the effect of the low flip angle pulses on loss of polarization using eq 7.

$$S = S_{\text{obs}} / (\cos\alpha)^n \quad (7)$$

where  $S$  is the corrected polarization,  $S_{\text{obs}}$  is the observed polarization,  $n$  is the number of the RF excitation pulses preceding the current observation, and  $\alpha$  is the pulse flip angle.

The simple two-site exchange analysis was, however, inadequate since there was an increase in the echo intensity, relative to the FID intensity, during the exchange time course, which implied a change in the distribution of the observed lactate species. Therefore, a second kinetic analysis was performed using the echo/FID (EF) ratios and in which the two-site exchange model was modified to include an inflow term. By using the EF ratio the effects of the RF pulses and  $T_1$  relaxation on the polarization were minimized and consequently ignored in this analysis. For perdeuterated lactate ( $L-[1-^{13}\text{C}, \text{U}-^2\text{H}]$ -lactate) this model can be written as:



where  $k_I \text{EF}_I$  represents the inflow term and  $\text{EF}_{\text{DL}}$  and  $\text{EF}_{\text{HL}}$  represent respectively the detected C2-deuterated and C2-protonated lactate within the tumor. The differential equations for this system can be written in matrix form as:

$$\begin{bmatrix} \text{EF}_{\text{DL}} \\ \text{EF}_{\text{HL}} \\ \text{EF}_I \end{bmatrix}_t = e^{\left( \begin{bmatrix} -k_{\text{DH}} & k_{\text{HD}} & k_I \\ k_{\text{DH}} & -k_{\text{HD}} & 0 \\ 0 & 0 & -k_I \end{bmatrix} t \right)} \begin{bmatrix} \text{EF}_{\text{DL}} \\ \text{EF}_{\text{HL}} \\ \text{EF}_I \end{bmatrix}_0 \quad (9)$$

The measured values of  $\text{EF}_{\text{DL}}$  and  $\text{EF}_{\text{HL}}$  were fitted to the model to obtain the exchange rate constants  $k_{\text{DH}}$ ,  $k_{\text{HD}}$  and the inflow term  $k_I \text{EF}_I$ .

## RESULTS AND DISCUSSION

The  $^{13}\text{C}$ - $^1\text{H}$   $J$  coupling constants between the C1 carbon and the C2 proton and between the C1 carbon and the C3 protons in lactate have been reported as 3.3 and 4.1 Hz, respectively.<sup>21</sup> These were confirmed from spectra of  $L-[1-^{13}\text{C}_1]$ lactate (Figure 1) and  $L-[1-^{13}\text{C}_1, 2-^2\text{H}]$ lactate (data not shown). In a heteronuclear  $^{13}\text{C}/^1\text{H}$  spin-echo experiment with  $L-[1-^{13}\text{C}_1]$ -lactate at thermal equilibrium, inversion of the  $^{13}\text{C}$  signal is observed at an echo time (TE) of  $\sim 310$  ms ( $1/J_{1,^{13}\text{C}, 2-^1\text{H}}$ ) when a selective  $180^\circ$  proton pulse is applied at the resonant frequency of the C2 proton (4.11 ppm), whereas no inversion is observed with  $L-[1-^{13}\text{C}_1, \text{U}-^2\text{H}]$ lactate (Figure 2). Thus, by taking advantage of the relatively slow  $^{13}\text{C}$  spin-spin relaxation rate ( $R_2$ ), the presence of a deuterium label at the C2 position of lactate, which cannot be observed directly in the relatively poorly resolved  $^{13}\text{C}$  spectra obtained in vivo (Figure 3), can readily be detected from phase inversion of the spin-coupled C1  $^{13}\text{C}$  resonance in the spin-echo experiment. The effect of  $J$  coupling between the C1 carbon and the C3 protons is observed at TE  $\approx 250$  ms ( $1/J_{1,^{13}\text{C}, 3-^1\text{H}}$ ), where application of a selective  $180^\circ$  proton pulse at the resonant frequency of the C3 methyl protons (1.33 ppm) results in phase inversion of the C1  $^{13}\text{C}$  resonance (Figure 1B). The effect of this coupling between the C1 carbon and the C3 protons was removed in experiments performed in vivo by using perdeuterated lactate ( $[1-^{13}\text{C}, \text{U}-^2\text{H}]$ lactate), which also removed the requirement for frequency-selective proton pulses.

Injection of hyperpolarized  $[1-^{13}\text{C}]$ lactate into an EL4-tumor-bearing mouse resulted in a low level of detectable  $[1-^{13}\text{C}]$ pyruvate (Figure 3a), which peaked at  $\sim 2\%$  of the total



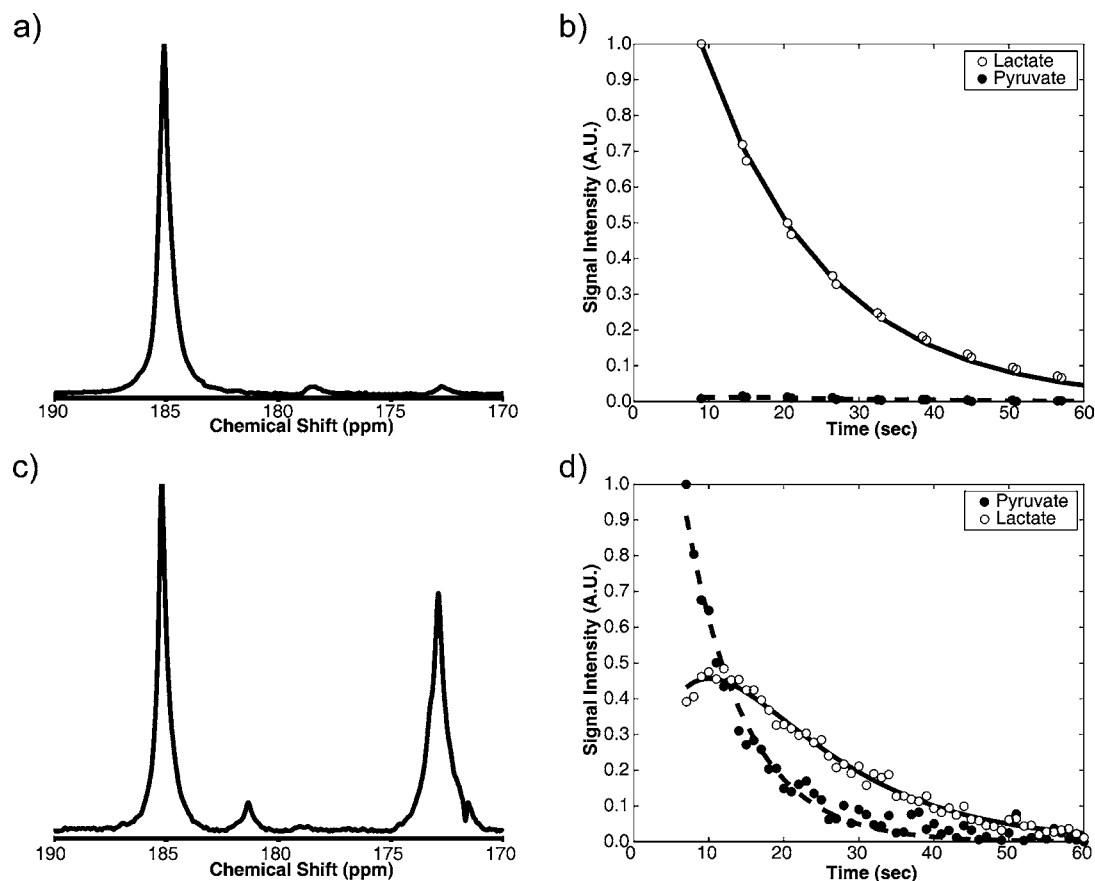


**Figure 3.** Pulse and acquire  $^{13}\text{C}$  spectra from an EL-4 tumor following i.v. injection of 60 mM hyperpolarized  $L$ -[1- $^{13}\text{C}$ ,U- $^2\text{H}$ ]lactate (a) or 75 mM [1- $^{13}\text{C}$ ]pyruvate (c). The lactate signal is at 185.08 ppm and the pyruvate signal at 172.9 ppm. There are also smaller signals from alanine at 178.48 ppm and pyruvate hydrate at 181 ppm. The corresponding time courses for label exchange between labeled lactate and pyruvate and between labeled pyruvate and lactate are shown in (b) and (d), respectively.

observable  $^{13}\text{C}$  signal (Figure 3b). Fitting of the lactate and pyruvate peak intensities to a two-site exchange model<sup>3</sup> gave a rate constant for flux of label from lactate to pyruvate of  $0.0009 \pm 0.0005 \text{ s}^{-1}$ . Contrast this with experiments with hyperpolarized [1- $^{13}\text{C}$ ]pyruvate where, for much of the exchange time course, the lactate peak intensity exceeded that of pyruvate (Figure 3c,d). Fitting of these data gave a rate constant for the exchange of  $0.056 \text{ s}^{-1}$ , which is comparable to values measured previously in this tumor model.<sup>3,22</sup>

Figure 4a shows the Fourier transformed FID (Figure 4a (i)) and echo signals (Figure 4a (ii)) obtained from an EL4 tumor following injection of  $L$ -[1- $^{13}\text{C}$ ]lactate into a tumor-bearing mouse, where the FID was measured immediately following the low flip angle pulse in a heteronuclear  $^{13}\text{C}/^1\text{H}$  spin-echo experiment, and the echo was measured at 310 ms. Alternate echoes were acquired with a  $180^\circ$   $^1\text{H}$  pulse, which resulted in nearly complete phase inversion of the spin-coupled hyperpolarized  $\text{C}_1$   $^{13}\text{C}$  resonance (Figure 4a (ii) and c). The average ratio of the echo signals obtained with and without the  $180^\circ$   $^1\text{H}$  pulse ( $H_+/H_-$ ) for each echo pair (see Methods section) was  $86 \pm 7\%$  when the loss of polarization between the pair of echoes was ignored and  $92 \pm 7\%$  when the echo signals were first corrected for this loss of polarization using the FID intensities obtained after each low flip angle pulse in the echo pair. Conversion of the echo intensities obtained with and without the  $180^\circ$   $^1\text{H}$  pulse ( $H_+/H_-$ ), using eqs 1 and 2, into the concentrations of the C2-deuterated and C2-protonated

lactate species gave, due to imperfect phase inversion, an artificial baseline for [1- $^{13}\text{C}$ ,2- $^2\text{H}$ ]lactate of  $\sim 10\%$ , when of course there was no deuterated lactate present (Figure 4e). This low but artificial baseline remained constant throughout the experiment (Figure 4g). In contrast, when  $L$ -[1- $^{13}\text{C}$ ,U- $^2\text{H}$ ]lactate was injected, there was initially little change in the hyperpolarized  $\text{C}_1$   $^{13}\text{C}$  resonance following application of a  $180^\circ$   $^1\text{H}$  pulse; however, as exchange of the C2 deuterium with C2 protons in the endogenous lactate pool proceeded, the  $180^\circ$   $^1\text{H}$  pulse resulted in a progressively larger decrease in the  $^{13}\text{C}$  resonance intensity (Figure 4d). Conversion of these signal intensities into the concentrations of the C2-deuterated ([1- $^{13}\text{C}_1$ ,U- $^2\text{H}$ ]) and C2-protonated ([1- $^{13}\text{C}_1$ ,2- $^1\text{H}$ ,3- $^2\text{H}_3$ ]) lactate species, using eqs 1 and 2, showed an increasing signal from the C2-protonated species during the exchange time course (Figure 4f,h). The exchange rate constants calculated using eq 5 are summarized in Table 1. Correction for the artificial baseline, due to imperfect phase inversion, had only a modest effect on the fitted values (eqs 3 and 4). The relative decrease in label flux after etoposide treatment was similar to that observed previously with [1- $^{13}\text{C}$ ]pyruvate in this tumor model.<sup>3,22</sup> The calculated relaxation rate ( $R_1$ ) from these three experiments was  $0.037 \pm 0.005 \text{ s}^{-1}$  ( $n = 3$ ) (Table 2).

The ratio of the FID intensity to the intensity of the echo decreased substantially such that by 45 s after lactate injection the amplitudes of the echo and FID were comparable

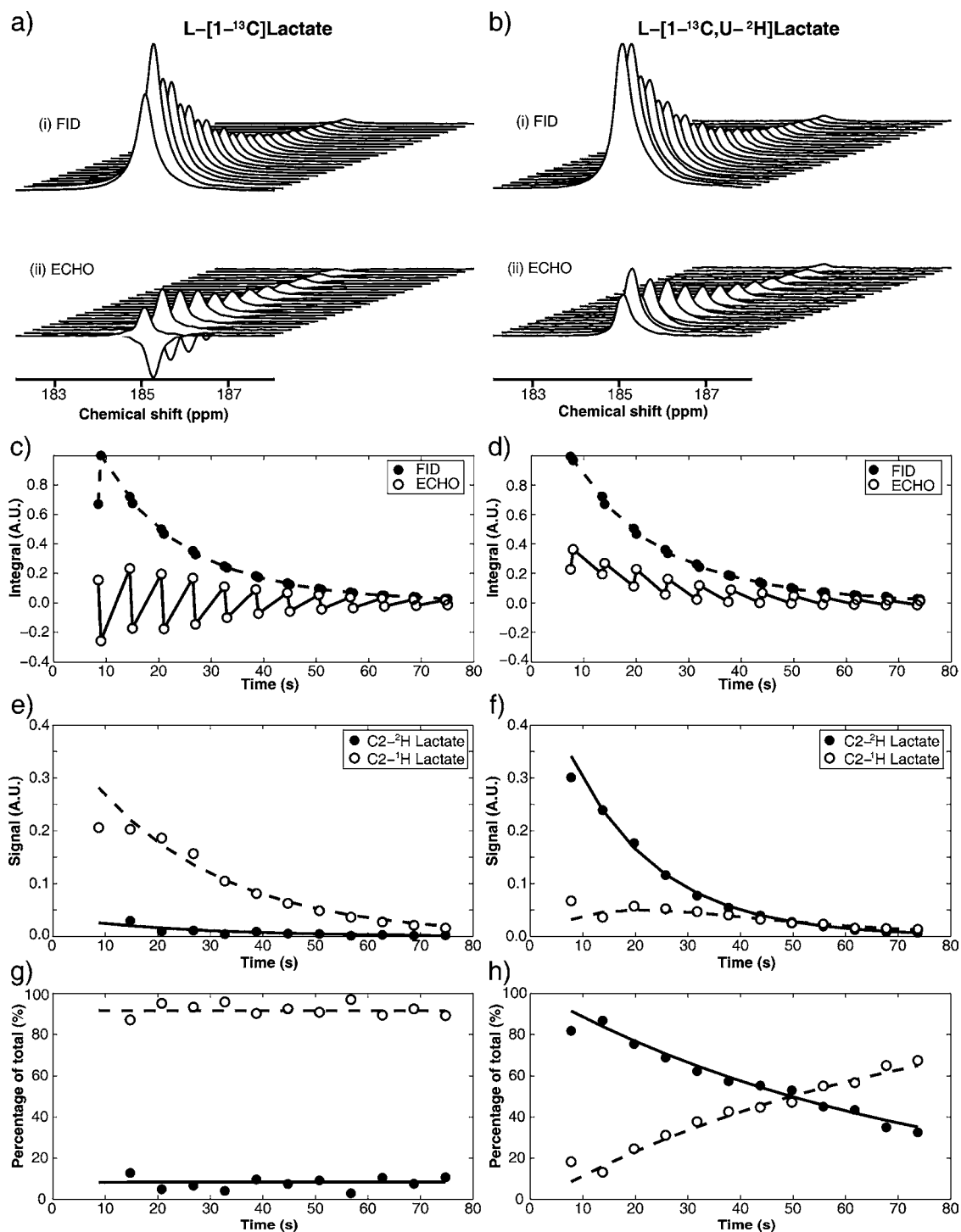


**Figure 4.** Detection of C2-protonated and C2-deuterated lactate species in a tumor in vivo using a heteronuclear spin-echo  $^{13}\text{C}/^1\text{H}$  experiment ( $\text{TE} = 310$  ms). Spectra (a (i) and (ii)) and data analysis (c, e, and g) following i.v. injection of hyperpolarized C2-protonated lactate ( $\text{L}-[1-^{13}\text{C}]\text{lactate}$ ). The spectra shown are the Fourier transformed FID, acquired 1 ms after the low flip angle pulse (a (i)), and the echoes (a (ii)), which were acquired with and without  $^1\text{H}$  inversion pulses. In this series the  $180^\circ$   $^1\text{H}$  pulses were applied in the order  $\text{H}_-/\text{H}_+$  (see Methods section). Corresponding spectra (b (i) and (ii)) and data analysis (d, f, and h) following i.v. injection of hyperpolarized C2-deuterated lactate ( $\text{L}-[1-^{13}\text{C},\text{U}-^2\text{H}]\text{lactate}$ ). In this series the  $180^\circ$   $^1\text{H}$  pulses were applied in the order  $\text{H}_+/\text{H}_-$  (see Methods section). Panels (c) and (d) show the FID and echo intensities with time (s) after lactate injection. Panels (e) and (f) show the calculated signal intensities due to the C2-protonated and C2-deuterated lactate species, and panels (g) and (h) show the percentages of these species as a fraction of the total lactate signal. The solid and dotted lines represent the best fit to the two-site exchange model (eq 5). The fitted exchange and relaxation rate constants are shown in Tables 1 and 2, respectively.

(Figures 4 c,d), indicating that at later time points we were detecting a single lactate pool with relatively long  $T_2$ .  $T_2$  measurements at  $\sim 80$  s postinjection gave an apparent  $T_2$

relaxation time of  $0.605 \pm 0.013$  s ( $n = 2$ ). In a previous study in this tumor model, where we injected hyperpolarized  $[1-^{13}\text{C}]\text{pyruvate}$ , we observed two  $T_2$  components for pyruvate;

**Table 1. Calculated Exchange Rates in Vivo Using Echo Intensities and the Two-Site Exchange Model and Using the Echo/FID (EF) Ratios and the Two-Site Exchange Model, Modified to Include an Inflow Term, Following Injection of L-[1-<sup>13</sup>C,U-<sup>2</sup>H]Lactate**

two-site exchange model (fit to echo intensities)	$k_{DH}$ (s <sup>-1</sup> )	$k_{HD}$ (s <sup>-1</sup> )
tumor 1 <sup>a</sup>	0.020	0.018
tumor 2 <sup>a</sup>	0.024	0.018
tumor 2, treated <sup>a</sup>	0.012	0

two-site exchange model, with an additional inflow term (fit to EF ratios)	$k_i$ (s <sup>-1</sup> )	$k_{DH}$ (s <sup>-1</sup> )	$k_{HD}$ (s <sup>-1</sup> )	EF <sub>i</sub>
tumor 1	0.062	0.032	0.019	0.635
tumor 2	0.069	0.052	0.062	0.558
tumor 2, treated	0.107	0.022	0.007	0.544

<sup>a</sup>The fitted  $R_1$  values from these experiments are shown, as an average, in Table 2.

a short component ( $0.12 \pm 0.02$  s,  $46 \pm 14\%$  of total signal) and a longer component ( $0.54 \pm 0.16$  s,  $62 \pm 22\%$  of total signal), where these measurements were made much earlier after injection (15 – 30 s). An interpretation of these results is that the short  $T_2$  component represents the blood pool, which has an apparently short  $T_2$  because of flow effects, and therefore that the relative increase in lactate echo amplitude observed here was due to inflow of lactate from the blood pool into the tumor extravascular space. Note that the  $T_1$ 's determined from the echo intensities are longer than those determined from the FID intensities (Table 2), which is also consistent with this notion. Note also that these changes in  $T_2$  had only a small effect on the degree of peak inversion since changing the sequence of the  $180^\circ$  <sup>1</sup>H pulses ( $H_+/H_-$  or  $H_-/H_+$ ) had no effect on the measured exchange kinetics, as would be expected from the relatively short echo spacing.

Reanalysis of the data shown in Figure 4 using the ratio of the FID intensity to the intensity of the echo (echo/FID ratio; EF) confirmed that this ratio increased over the exchange time course (Figure 5a,b). The concentrations of the different lactate species can be calculated from the EF ratios using eqs 1 and 2 and substituting for  $S_{DL}$ ,  $S_{HL}$ ,  $S_{H-}$ , and  $S_{H+}$  with the corresponding EF ratios. When this analysis was used for the case where C2-protonated lactate was injected (L-[1-<sup>13</sup>C]-lactate; Figure 5c), a progressive increase in the signal intensity from this lactate species was observed, which can be explained by inflow of the injected lactate into the tumor. These data and the EF values obtained following injection of deuterated lactate

(L-[1-<sup>13</sup>C,U-<sup>2</sup>H]lactate; Figure 5d) were fitted to eq 9 to obtain the exchange rate constants and a term representing lactate inflow (Table 1). As noted for Figure 4e,g, the apparent production of C2-deuterated lactate following injection of C2-protonated lactate is due to imperfect phase inversion. Deconvolution of the effects of flow, membrane transport, and LDH kinetics on the observed exchange will require measurements where the levels of the transporter or LDH have been modulated, for example by changing LDH expression using a PI3K inhibitor.<sup>7</sup>

The relaxation rates ( $R_1$ ,  $R_2$ ) for the polarization in the various lactate species, which were determined using pulse and acquire spectra and also from the FID and echo intensities in the heteronuclear spin–echo experiment, are shown in Table 2. The  $R_1$  relaxation rates calculated from the spin–echo experiments were faster than those calculated from the pulse and acquire spectra. This presumably reflects imperfections in the <sup>13</sup>C refocusing pulses, which were delivered using a surface coil, leading to an accelerated loss of  $z$  magnetization. However, FID intensities within each echo pair were similar (Figure 4c,d), showing that there was only minor loss of  $z$  magnetization between each echo pair.

The sensitivity of this experiment, in which tumor LDH activity was assessed by measuring exchange of the C2 deuterium with protons in endogenous lactate, was lower than that in which exchange was measured directly between [1-<sup>13</sup>C]pyruvate and endogenous lactate (Figure 3c,d) but exceeded that when exchange was measured between [1-<sup>13</sup>C]-lactate and endogenous pyruvate (Figure 3a,b). Consider the signal intensities at 10 s following injection, when the concentration of labeled lactate was at a maximum following injection of hyperpolarized [1-<sup>13</sup>C]pyruvate (Figure 3d). At this time point the lactate signal was ~50% of the injected pyruvate signal intensity (Figure 3d). At the same time point in the experiment with [1-<sup>13</sup>C<sub>1</sub>,U-<sup>2</sup>H]lactate the echo intensity was ~40% of the signal obtained immediately after the low flip angle pulse, due to  $T_2$  relaxation. Of this signal ~20% was due to the C2-protonated lactate (L-[1-<sup>13</sup>C<sub>1</sub>,3-<sup>2</sup>H<sub>3</sub>]lactate (Figure 4f), or ~10% of the lactate signal that was observed immediately after the low flip angle pulse. Contrast this with the experiment where exchange was measured between L-[1-<sup>13</sup>C]lactate and endogenous pyruvate, where the pyruvate signal was only ~2% of the signal from injected lactate (Figure 3b).

**Table 2. Apparent Spin–Lattice ( $R_1$ ) and Spin–Spin ( $R_2$ ) Relaxation Rates for the Different Labeled Lactate Species in Vitro and in a Tumor in Vivo**

	L-[1- <sup>13</sup> C,U- <sup>2</sup> H]lactate (s <sup>-1</sup> )	L-[1- <sup>13</sup> C,3- <sup>2</sup> H <sub>3</sub> ]lactate (s <sup>-1</sup> )	L-[1- <sup>13</sup> C]lactate (s <sup>-1</sup> )
$R_1$			
in vitro <sup>a</sup>	$0.021 \pm 0.002$	$0.020 \pm 0.001$	$0.023 \pm 0.001$
in vivo, pulse-acquire	0.023	0.025	0.035
in vivo, spin–echo (FID)	$0.047 \pm 0.002$ ( $n = 3$ )	0.042	0.054
in vivo, spin–echo (echo)	$0.037 \pm 0.005$ ( $n = 3$ )	–	0.038
$R_2$			
in vitro <sup>b</sup>	$0.75 \pm 0.06$ ( $n = 4$ )	–	$0.67 \pm 0.06$ ( $n = 4$ )

<sup>a</sup>Measured with non-hyperpolarized samples of 30 mM lactate at 37 °C in phosphate-buffered saline, pH 7.1, 1 mM EDTA using an inversion–recovery pulse sequence. These values are from single measurements, and the quoted errors are on the fit. <sup>b</sup>Measured with non-hyperpolarized samples of 10 mM lactate at 25 °C in <sup>2</sup>H<sub>2</sub>O.

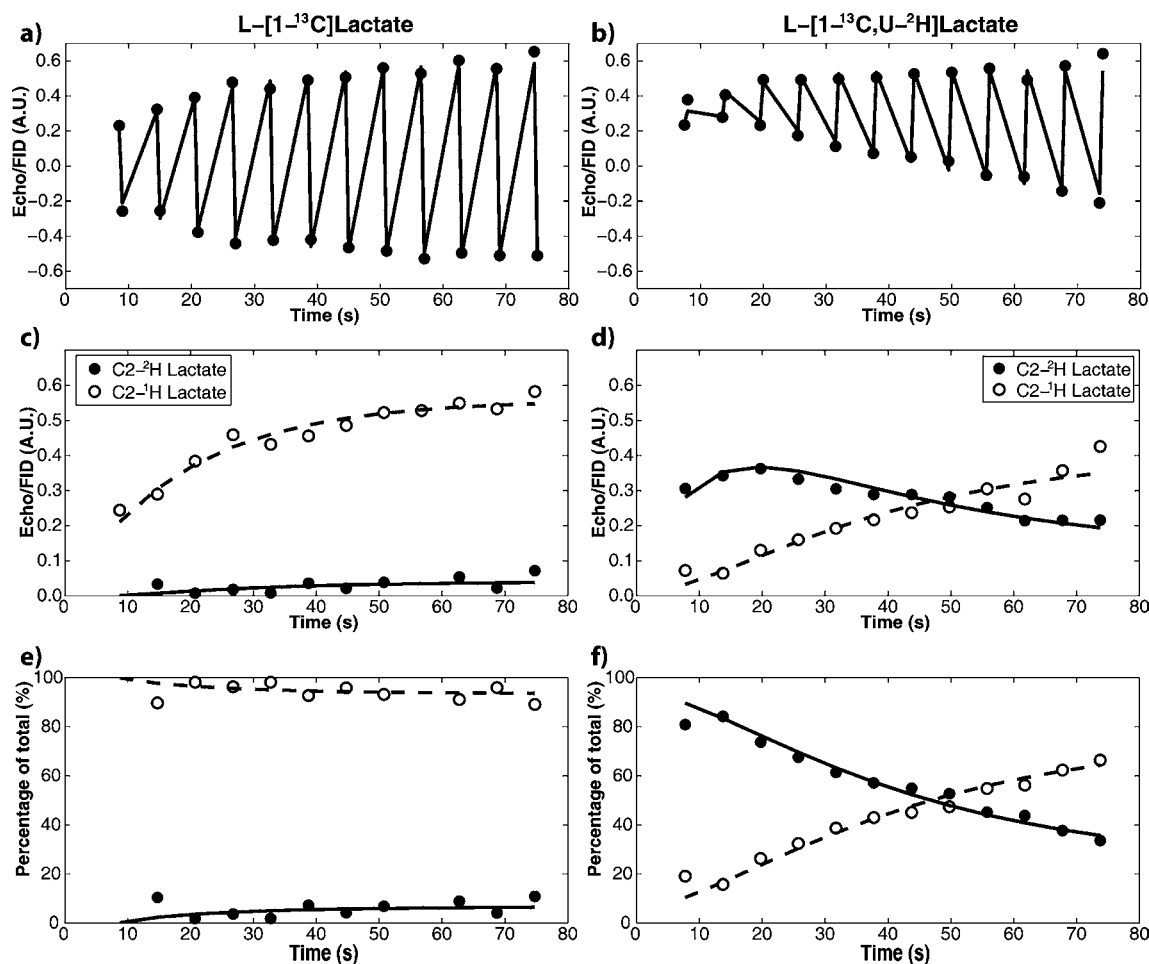


**Figure 5.** Analysis of the data shown in Figure 4 using the echo/FID ratios. Panels (a) and (b) show the echo/FID ratios obtained following injection of C2-protonated (L-[1-<sup>13</sup>C]lactate) and C2-deuterated lactate (L-[1-<sup>13</sup>C,U-<sup>2</sup>H<sub>3</sub>]lactate) respectively. Panels (c) and (d) show the calculated echo/FID ratios for the C2-protonated and C2-deuterated lactate species. Panels (e) and (f) show the concentrations of the C2-protonated and C2-deuterated lactate species as a fraction of the total injected lactate. The solid and dotted lines represent the best fit to the two-site exchange model, which has been modified to include lactate inflow (eq 9). The fitted exchange rate constants are shown in Table 1.

## CONCLUSIONS

We have described a new hyperpolarized substrate, L-[1-<sup>13</sup>C,U-<sup>2</sup>H]lactate, in which measurements of exchange of the C2 deuterium with the C2 protons in endogenous lactate, in a hyperpolarized <sup>13</sup>C/<sup>1</sup>H heteronuclear spin-echo experiment, can be used to probe LDH kinetics in vivo. This experiment has the advantage that it uses lactate, which can be injected at physiological concentrations, and is more sensitive than in the experiment in which exchange of the <sup>13</sup>C label between lactate and pyruvate is measured, where the size of the endogenous pyruvate pool is a limiting factor. In addition, since only a single peak is observed, imaging will be more straightforward since chemical shift selection is not required. Furthermore, at the lower magnetic field strengths used in the clinic, the T<sub>2</sub> relaxation times should be longer, and therefore detection of the C2-protonated and C2-deuterated lactate species should be more sensitive.

## AUTHOR INFORMATION

### Corresponding Author

kmb1001@cam.ac.uk

## Notes

The authors declare the following competing financial interest(s): Research support from GE Healthcare.

## ACKNOWLEDGMENTS

This work was supported by a Cancer Research UK Program Grant to K.M.B. (C197/A3514) and by a Translational Research Program Award from The Leukemia and Lymphoma Society. B.W.C.K. was in receipt of a Cancer Research UK studentship.

## REFERENCES

- (1) Kurhanewicz, J.; Vigneron, D.; Brindle, K.; Chekmenev, E.; Comment, A.; Cunningham, C.; DeBerardinis, R.; Green, G.; Leach, M.; Rajan, S.; Rizi, R.; Ross, B.; Warren, W.; Malloy, C. *Neoplasia* **2011**, *13*, 81–97.
- (2) Brindle, K. M.; Bohndiek, S. E.; Gallagher, F. A.; Kettunen, M. I. *Magn. Reson. Med.* **2011**, *66*, 505–519.
- (3) Day, S. E.; Kettunen, M. I.; Gallagher, F. A.; Hu, D. E.; Lerche, M.; Wolber, J.; Golman, K.; Ardenkjaer-Larsen, J. H.; Brindle, K. M. *Nat. Med.* **2007**, *13*, 1382–1387.
- (4) Ward, C. S.; Venkatesh, H. S.; Chaumeil, M. M.; Brandes, A. H.; Vancrackinge, M.; Dafni, H.; Sukumar, S.; Nelson, S. J.; Vigneron, D. B.;



Kurhanewicz, J.; James, C. D.; Haas-Kogan, D. A.; Ronen, S. M. *Cancer Res.* **2009**, *70*, 1296–1305.

(5) Albers, M. J.; Bok, R.; Chen, A. P.; Cunningham, C. H.; Zierhut, M. L.; Zhang, V. Y.; Kohler, S. J.; Tropp, J.; Hurd, R. E.; Yen, Y. F.; Nelson, S. J.; Vigneron, D. B.; Kurhanewicz, J. *Cancer Res.* **2008**, *68*, 8607–8615.

(6) Veech, R. L.; Lawson, J. W.; Cornell, N. W.; Krebs, H. A. *J. Biol. Chem.* **1979**, *254*, 6538–6547.

(7) Witney, T. H.; Kettunen, M. I.; Brindle, K. M. *J. Biol. Chem.* **2011**, *286*, 24572–24580.

(8) Kettunen, M. I.; Hu, D.-E.; Witney, T. H.; McLaughlin, R.; Gallagher, F. A.; Bohndiek, S. E.; Day, S. E.; Brindle, K. M. *Magn. Reson. Med.* **2010**, *63*, 872–880.

(9) Koukourakis, M. I.; Giatromanolaki, A.; Sivridis, E.; Bougioukas, G.; Didilis, V.; Gatter, K. C.; Harris, A. L. *Br. J. Cancer* **2003**, *89*, 877–885.

(10) Riches, A.; Sharp, J.; Brynmor Thomas, D.; Vaughan Smith, S. *J. Physiol.* **1973**, *228*, 279–284.

(11) Wu, C.; Okar, D. A.; Newgard, C. B.; Lange, A. J. *J. Clin. Invest.* **2001**, *107*, 91–98.

(12) Kelly, F.; Simonsen, D.; Elman, R. *J. Clin. Invest.* **1948**, *27*, 795–804.

(13) Marbach, E. P.; Weil, M. H. *Clin. Chem.* **1967**, *13*, 314–325.

(14) Hurley, B. F.; Hagberg, J. M.; Allen, W. K.; Seals, D. R.; Young, J. C.; Cuddihy, R. W.; Holloszy, J. O. *J. Appl. Physiol.* **1984**, *56*, 1260–1264.

(15) Chen, A. P.; Kurhanewicz, J.; Bok, R.; Xu, D.; Joun, D.; Zhang, V.; Nelson, S. J.; Hurd, R. E.; Vigneron, D. B. *Magn. Reson. Imaging* **2008**, *26*, 721–726.

(16) Brindle, K. M.; Campbell, I. D.; Simpson, R. J. *Eur. J. Biochem.* **1986**, *158*, 299–305.

(17) Brindle, K. M.; Brown, F. F.; Campbell, I. D.; Foxall, D. L.; Simpson, R. J. *Biochem. J.* **1982**, *202*, 589–602.

(18) Brindle, K. M.; Brown, F. F.; Campbell, I. D.; Grathwohl, C.; Kuchel, P. W. *Biochem. J.* **1979**, *180*, 37–44.

(19) Hohorst, H. In *Methods of Enzymatic Analysis*; Bergmeyer, H. U., Ed.; Verlag Chemie: Weinheim, 1970; Vol. 2, pp 1425–1429.

(20) Tannús, A.; Garwood, M. *NMR Biomed.* **1997**, *10*, 423–434.

(21) Chen, A. P.; Tropp, J.; Hurd, R. E.; Crieckinge, M. V.; Carvajal, L. G.; Xu, D.; Kurhanewicz, J.; Vigneron, D. B. *J. Magn. Reson.* **2009**, *197*, 100–106.

(22) Witney, T.; Kettunen, M.; Day, S.; Hu, D.; Neves, A.; Gallagher, F.; Fulton, S.; Brindle, K. *Neoplasia* **2009**, *6*, 574–582.